JCTC Journal of Chemical Theory and Computation

ARTICLE

pubs.acs.org/JCTC

# A Simple Algorithm for Determining Orthogonal, Self-Consistent Excited-State Wave Functions for a State-Specific Hamiltonian: Application to the Optical Spectrum of the Aqueous Electron

Leif D. Jacobson and John M. Herbert*

Department of Chemistry, The Ohio State University, Columbus, Ohio 43210, United States

**ABSTRACT:** We recently introduced a mixed quantum/classical model for the hydrated electron that includes electron/water polarization in a self-consistent fashion, using a polarizable force field for the water molecules [ *J. Chem. Phys.* **2010**, *133*, 154506]. Calculation of the electronic absorption spectrum for this model is not straightforward, owing to the state-specific nature of the Hamiltonian, the high density of electronic states, and the large solvent polarization response upon electronic excitation. Together, these properties make it difficult or impossible to converge the polarizable solvent dipoles self-consistently for each excited-state wave function. Here, we overcome this problem by means of an extended Lagrangian procedure for performing constrained annealing in the space of electronic variables. By construction, this algorithm affords self-consistent, mutually orthogonal solutions for any state-specific Hamiltonian, and we illustrate this approach by computing the optical spectrum of our polarizable model for the aqueous electron. The spectrum thus obtained affords better agreement with experiment than previous, perturbative calculations of solvent dipole relaxation. Strengths, weaknesses, and possible generalizations of this procedure are discussed.

## I. INTRODUCTION

First observed directly in 1962,[1] the aqueous (or hydrated) electron, $e^-(aq)$, has since that time been the subject of numerous experimental and theoretical investigations.[2,3] Despite numerous atomistic simulations of this species over the past 25 years,[3] it was not until quite recently that the Lorentzian decay on the high-energy side of the optical absorption spectrum was reproduced even qualitatively.[4,5]

Due to the highly quantum mechanical nature of the solute (an electron), the dynamics and the bulk structure of $e^-(aq)$ have mostly been studied using one-electron pseudopotential methods,[3,6−9] in other words, hybrid quantum mechanics/molecular mechanics (QM/MM) procedures with an one-electron QM region. The ostensible simplicity of such models (only one QM electron), combined with the importance of $e^-(aq)$ in the radiation chemistry of aqueous systems,[2,10,11] means that these one-electron pseudopotential models have historically been used to test a variety of mixed quantum/classical simulation techniques.

We have recently developed a new one-electron pseudopotential model that incorporates self-consistent polarization between the solvent (water) and the single "excess" electron.[5] Results from this model compare favorably to ab initio calculations in $(H_2O)_n^-$ clusters, and various properties of the bulk species, $e^-(aq)$, are also reproduced reasonably well.[5] Our model utilizes the AMOEBA water potential,[12] which treats polarization by means of inducible point dipoles located on each MM atom. In our hydrated electron model,[5,13] the electric field generated by the QM wave function contributes to the total electric field that polarizes these dipoles.

Because the induced dipoles represent electronic degrees of freedom, they should respond (polarize) on the time scale of electronic excitation. As such, it seems physically reasonable that the calculation of excited states in our polarizable model should require a self-consistent calculation in which the solvent dipoles are converged with respect to each excited-state wave function. Because the QM Hamiltonian depends on the inducible dipoles, the realization of such a procedure effectively renders the Hamiltonian state specific, i.e., the nature of the Hamiltonian depends upon the particular electronic state that one is attempting to calculate.

In previous work,[5] we encountered difficulties in obtaining self-consistent, excited-state solutions to this effective Hamiltonian, owing to the fact that the energy gaps between states are small (∼0.1 eV), while the electronic relaxation energy of the solvent is large (e.g., 1.4 eV for vertical electron detachment in the bulk limit).[5] This leads to frequent state switching during the wave function/dipole optimization. Even if we were able to converge the excited-state wave functions self-consistently with the induced dipoles, the wave functions thus obtained would not be mutually orthogonal, owing to the state-specific nature of the effective Hamiltonian. In view of these difficulties, we have previously resorted to the use of a perturbative correction for the solvent's polarization response upon excitation of the wave function.[4,5] While this approach allowed us to make progress in understanding the role of solvent polarization, it suffers from a lack of mutual orthogonality among the excited-state wave functions, owing to the state-specific nature of the perturbation. As such, one might reasonably be concerned about possible artifacts in the predicted oscillator strengths.

Here, we report a simulated annealing procedure in the space of electronic variables (wave function amplitudes and induced dipoles) by means of which the classical dipoles are converged self-consistently with respect to each wave function. In addition, our algorithm employs Lagrange multipliers to ensure that all of

**Received:** April 16, 2011
**Published:** June 13, 2011

the wave functions are orthonormal, despite the state-specific nature of the Hamiltonian. As a numerical demonstration of this procedure, we calculate the electronic absorption spectrum of the aqueous electron, using our polarizable one-electron model. The orthogonality issue is general to QM/MM methods that employ polarizable force fields, and therefore these ideas may be more broadly applicable. (However, the large polarization energies that we encounter may be unique to charged systems.)

Orthogonality is also an issue in certain self-consistent field (SCF) methods. For example, Gill and co-workers[14,15] have recently introduced a maximum overlap method (MOM) that attempts to find excited-state solutions to the SCF equations by choosing the occupied orbitals at each SCF iteration, not in the usual aufbau way but rather by selecting those molecular orbitals that have the largest overlap with a set of user-specified guess orbitals. This situation is similar to the problem outlined above in that the effective Hamiltonian (Fock matrix) is state specific, and the excited-state solutions are not mutually orthogonal. Moreover, there is a direct correspondence between our polarizable QM/MM method and the SCF method. In the QM/MM procedure, we use the one-electron density, $|\psi|^2$, to compute induced dipoles, then use these dipoles to construct an effective Hamiltonian and finally diagonalize this Hamiltonian to obtain a new density. This process is iterated to self-consistency. In the SCF method, one uses the density to compute a new Fock matrix. We believe that our algorithm can be modified for use in the SCF procedure, in a manner that is conceptually (if not computationally) straightforward, and we hope to report on this in the future.

This paper is organized as follows: Section II provides a brief overview of our one-electron pseudopotential model for $e^-(aq)$ and introduces the electronic annealing method. Details of the calculations are given in Section III. In Section IV, we present results for the optical absorption spectrum of $e^-(aq)$ and draw a comparison with results obtained previously, using a perturbative treatment of the solvent's polarization response. We discuss certain formal aspects of the method, and some possible generalizations, in Section V. Section VI provides a summary.

## II. THEORY

**A. Polarizable QM/MM Model.** We will not discuss our hydrated electron model in detail but will only highlight those aspects that are important to understand the annealing procedure. As in many polarizable QM/MM models, the total Hamiltonian in our model is a function of both the coordinates of the MM atoms, $\{\vec{R}_i\}$, as well as the induced MM dipoles, $\{\vec{\mu}_i\}$. The one-electron Hamiltonian can be written

$$\hat{H}(\{\vec{\mu}_i\},\{\vec{R}_i\}) = \hat{T} + V_{elec-water}(\{\vec{\mu}_i\},\{\vec{R}_i\}) + V_{MM}(\{\vec{\mu}_i\},\{\vec{R}_i\}) \quad (1)$$

Here, $\hat{T}$ is the one-electron kinetic energy operator, $V_{\mathrm{elec-water}}$ is the electron−water pseudopotential, and $V_{\mathrm{MM}}$ is the molecular mechanics (MM) potential energy function for the polarizable water molecules. In our model, $V_{\mathrm{MM}}$ is the AMOEBA water force field.[12] The pseudopotential, $V_{\mathrm{elec-water}}$, contains electrostatic interactions between the electron and both the permanent and the induced multipole moments of the water molecules. In addition, it contains a repulsive potential that keeps the electron from collapsing into the core molecular region.

The induced dipoles are obtained by solution of the equation:[5,13]

$$\vec{\mu}_i = \alpha_i(\vec{F}_i^{MM} + \vec{F}_i^{QM}) \quad (2)$$

in which $\alpha_i$ is an (isotropic) polarizability for site $i$, $\vec{F}_i^{\mathrm{MM}}$ is the electric field produced by the MM subsystem at site $i$, and $\vec{F}_i^{\mathrm{QM}}$ is the electric field due to the wave function, also evaluated at site $i$. It can be shown that the induced dipoles defined by eq 2 minimize the total energy with respect to variations in $\vec{\mu}_i$.[13,16] The one-electron wave function is determined by the solution of the Schrödinger equation:

$$\hat{H}(\{\vec{\mu}_i\},\{\vec{R}_i\})|\psi\rangle = E|\psi\rangle \quad (3)$$

In practice, $|\psi\rangle$ is replaced by $\mathbf{c}$, a vector of amplitudes on a real-space grid. In order to obtain self-consistent polarization, we iterate eqs 2 and 3 to self-consistency. This procedure works well for the ground state but is difficult to converge for more than one or two excited states.

As a result of this difficulty we have, in previous work, computed approximate excited states by means of a simple perturbative scheme.[4,5] To define the perturbation, we first calculate the ground-state wave function $|\psi_0\rangle$ and some number of excited state wave functions, $|\psi_n\rangle$, using dipoles $\{\vec{\mu}_i^{(0)}\}$ that are converged with respect to $|\psi_0\rangle$. For each excited state, we then obtain new dipoles, $\{\vec{\mu}_i^{(n)}\}$, that are converged with respect to $|\psi_n\rangle$, without relaxing $|\psi_n\rangle$. The quantity

$$\hat{W}_n = \hat{H}(\{\vec{\mu}_i^{(n)}\},\{\vec{R}_i\}) - \hat{H}(\{\vec{\mu}_i^{(0)}\},\{\vec{R}_i\}) \quad (4)$$

serves as the perturbation.[4,5]

The perturbatively corrected wave functions thus obtained are not orthogonal, because the perturbation is state specific. However, they do turn out to be *approximately* orthogonal, with typical overlaps on the order of ∼0.1. Similar overlaps have been reported in MOM-SCF calculations, yet oscillator strengths in these calculations are in reasonable agreement with benchmark results.[14] As such, we believe that the $e^-(aq)$ spectra computed using the perturbative approach are at least qualitatively correct.

**B. Electronic Annealing Procedure.** We next describe our new algorithm to determine orthogonal excited states for state-specific effective Hamiltonians. The idea is not entirely new and is inspired by the Car−Parrinello molecular dynamics (CPMD) method,[17,18] wherein the electronic degrees of freedom are propagated dynamically as classical variables. The CPMD approach can also be used to obtain ground-state, single-determinant wave functions by clamping the nuclei in place and "annealing" a guessed wave function.[17,19] This amounts to a systematic removal of the fictitious kinetic energy associated with the electronic degrees of freedom. So far as we are aware, however, this technique has not been applied to the annealing of excited states. The main difference here, apart from the obvious difference of having only one QM electron in the present implementation, is that we constrain the wave function of interest to be orthogonal to each previously determined wave function. Doing this allows one to "march up" the manifold of excited states. Each excited state will then be defined as the lowest energy state that is orthogonal to all previously determined states. In a sense, this is a natural generalization of the linear variation method in elementary quantum mechanics.

Let $\mathbf{c}_0$ denote the vector of wave function amplitudes that we are interested in optimizing, and let $\{\mathbf{c}_i\}_{i=1}^{N}$ denote a set of

previously determined states. Note that $\mathbf{c}_0$ need not (and probably does not) represent the ground state, but the notation for the equations of motion will be simpler if we adopt a common index for all of the vectors. Only $\mathbf{c}_0$ is propagated in time, whereas $\mathbf{c}_1$, ..., $\mathbf{c}_N$ are fixed. We also find it convenient to define a dot product

$$\mathbf{c}_i \cdot \mathbf{c}_j = \langle \psi_i | \psi_j \rangle = \sum_{\mu=1}^{N_{grid}} c_{i,\mu} c_{j,\mu} \Delta\tau \tag{5}$$

where the sum runs over grid points and $\Delta\tau$ is the volume element defined by the cubic grid.

We insist that the new state, $\mathbf{c}_0$, be orthogonal to the previously determined states $\mathbf{c}_1$, ..., $\mathbf{c}_N$. Our method employs a Lagrangian

$$\mathscr{L} = \frac{1}{2}\tilde{m}_{el}\dot{\mathbf{c}}_0 \cdot \dot{\mathbf{c}}_0 + \frac{1}{2}\lambda_0(\mathbf{c}_0 \cdot \mathbf{c}_0 - 1) + \sum_{i=1}^{N} \lambda_i(\mathbf{c}_i \cdot \mathbf{c}_0) - E[\mathbf{c}_0, \{\vec{\mu}_i\}, \{\vec{R}_i\}] \tag{6}$$

where the $\lambda_i$ are the undetermined multipliers that enforce orthonormality constraints. The parameter $\tilde{m}_{el}$ is a fictitious electron mass, and $E[\mathbf{c}_0, \{\vec{\mu}_i\}, \{\vec{R}_i\}]$ is the energy functional. In principle, one could also propagate the induced dipoles dynamically. Because updating the Hamiltonian is far more expensive than minimizing the energy with respect to the induced dipoles, however, we choose to converge the dipoles each time $\mathbf{c}_0$ is updated.

From the Lagrangian in eq 6, one obtains the following equations of motion:

$$\tilde{m}_{el}\ddot{\mathbf{c}}_0 = -2\mathbf{H}\mathbf{c}_0 + \sum_{i=0}^{N} \lambda_i \mathbf{c}_i \tag{7}$$

Here, and in what follows, we use $\mathbf{H}$ to denote the Hamiltonian matrix, and for convenience we omit from our notation the explicit dependence of $\mathbf{H}$ on $\{\vec{\mu}_i\}$ and $\{\vec{R}_I\}$. In deriving eq 7, we have assumed that all quantities are real valued.

In the limit that the fictitious kinetic energy goes to zero, minimizing $\mathscr{L}$ with respect to $\mathbf{c}_0$ is equivalent to solving the time-independent Schrödinger equation. Therefore, if we propagate the electronic degrees of freedom according to eq 7 and systematically remove kinetic energy, we should eventually find a local minimum where $\partial\mathscr{L}/\partial\mathbf{c}_0 = 0$, although this minimum certainly need not be the global minimum. To remove kinetic energy, we add a velocity-dependent friction term to the equations of motion. Equation 7 is thereby modified, affording

$$\tilde{m}_{el}\ddot{\mathbf{c}}_0 = -2\mathbf{H}\mathbf{c}_0 + \sum_{i=0}^{N} \lambda_i \mathbf{c}_i - \gamma\tilde{m}_{el}\dot{\mathbf{c}}_0 \tag{8}$$

The friction parameter, $\gamma$, has dimensions of reciprocal time. This modified equation of motion is not conservative and does not arise from any Hamiltonian.

We next develop our algorithm for propagating the equations of motion in eq 8. For this we use a modified form of the velocity Verlet (VV) algorithm[20] and follow closely the work and the notation of Tuckerman and Parrinello,[21] who developed a VV-type algorithm to integrate the CPMD equations of motion. In the case of no damping ($\gamma = 0$), the appropriate VV equations for our purpose are

$$\mathbf{c}_0(t+\delta t) = \mathbf{c}_0(t) + \delta t\dot{\mathbf{c}}_0(t) + \frac{(\delta t)^2}{2\tilde{m}_{el}}\mathbf{f}(t) + \frac{(\delta t)^2}{2\tilde{m}_{el}}\sum_{i=0}^{N}\lambda_i^{\mathrm{R}}\mathbf{c}_i(t) \tag{9a}$$

$$\dot{\mathbf{c}}_0\left(t+\frac{1}{2}\delta t\right) = \dot{\mathbf{c}}_0(t) + \frac{\delta t}{2\tilde{m}_{el}}\mathbf{f}(t) + \frac{\delta t}{2\tilde{m}_{el}}\sum_{i=0}^{N}\lambda_i^{\mathrm{R}}\mathbf{c}_i(t) \tag{9b}$$

$$\dot{\mathbf{c}}_0(t+\delta t) = \dot{\mathbf{c}}_0\left(t+\frac{1}{2}\delta t\right) + \frac{\delta t}{2\tilde{m}_{el}}\mathbf{f}(t+\delta t) + \frac{\delta t}{2\tilde{m}_{el}}\sum_{i=0}^{N}\lambda_i^{\mathrm{V}}\mathbf{c}_i(t+\delta t) \tag{9c}$$

Here, $\delta t$ is the time step, and $\mathbf{f}(t) = -2\mathbf{H}\,\mathbf{c}_0(t)$ is the force on $\mathbf{c}_0$ at time $t$. Although we have written all of the vectors $\mathbf{c}_i$ as functions of time (in order to use a common index for $\mathbf{c}_0$ and $\mathbf{c}_i$, which facilitates a compact notation), the vectors $\{\mathbf{c}_i\}_{i=1}^{N}$ are fixed, and only $\mathbf{c}_0$ is propagated forward in time. In other words

$$\mathbf{c}_{i\neq 0}(t) = \mathbf{c}_{i\neq 0}(t+\delta t) \tag{10}$$

As in the RATTLE method,[22] the undetermined multipliers in eqs 9a−9c are allowed to have two different values, $\lambda_i^{\mathrm{R}}$ and $\lambda_i^{\mathrm{V}}$, representing coordinate and velocity constraints, respectively. This is similar to the approach used to maintain orthonormality constraints when integrating the CPMD equations of motion.[21]

Upon substituting $\mathbf{f}(t) \rightarrow \mathbf{f}(t) - \gamma\,\tilde{m}_{el}\dot{\mathbf{c}}_0(t)$ in eqs 9a−9c, one obtains equations for the case of finite damping. The corresponding VV algorithm can be expressed in three steps. The first step consists of both "coordinate" ($\tilde{\mathbf{c}}_0$) and half-step "velocity" ($\dot{\tilde{\mathbf{c}}}_0$) updates:

$$\tilde{c}_0(t+\delta t) = \mathbf{c}_0(t) + \delta t\left(1 - \frac{1}{2}\gamma\delta t\right)\dot{\mathbf{c}}_0(t) + \frac{(\delta t)^2}{2\tilde{m}_{el}}\mathbf{f}(t) \tag{11a}$$

$$\dot{\tilde{c}}_0\left(t+\frac{1}{2}\delta t\right) = \left(1 - \frac{1}{2}\gamma\delta t\right)\dot{\mathbf{c}}_0(t) + \frac{\delta t}{2\tilde{m}_{el}}\mathbf{f}(t) \tag{11b}$$

The second step consists of corrections:

$$\mathbf{c}_0(t+\delta t) = \tilde{\mathbf{c}}_0(t+\delta t) + \sum_{i=0}^{N} X_i\mathbf{c}_i(t) \tag{12a}$$

$$\dot{\mathbf{c}}_0\left(t+\frac{1}{2}\delta t\right) = \dot{\tilde{\mathbf{c}}}_0\left(t+\frac{1}{2}\delta t\right) + \sum_{i=0}^{N}\frac{X_i}{\delta t}\mathbf{c}_i(t) \tag{12b}$$

where the intermediate quantities $X_i$ are defined below. The final step is an update and a correction:

$$\dot{\tilde{\mathbf{c}}}_0(t+\delta t) = \left(1 + \frac{1}{2}\gamma\delta t\right)^{-1}\left[\dot{\mathbf{c}}_0\left(t+\frac{1}{2}\delta t\right) + \frac{\delta t}{2\tilde{m}_{el}}\mathbf{f}(t+\delta t)\right] \tag{13a}$$

$$\dot{\mathbf{c}}_0(t+\delta t) = \dot{\tilde{\mathbf{c}}}_0(t+\delta t) + \sum_{i=0}^{N} Y_i\mathbf{c}_i(t+\delta t) \tag{13b}$$

Equations 12a, 12b, 13a and 13b employ the intermediate quantities:

$$X_i = \frac{(\delta t)^2}{2\tilde{m}_{el}}\lambda_i^{\mathrm{R}} \tag{14}$$

and

$$Y_i = \frac{\delta t}{2\tilde{m}_{el}}\left(1+\frac{1}{2}\gamma\delta t\right)^{-1}\lambda_i^{V} \tag{15}$$

The values of $X_i$ and $Y_i$ are chosen to satisfy the constraint equations:

$$\mathbf{c}_0\cdot\mathbf{c}_0 = 1 \tag{16a}$$

$$\mathbf{c}_0\cdot\mathbf{c}_{i\neq 0} = 0 \tag{16b}$$

We start by substituting the first update of the second step of the algorithm, eq 12a, into these constraint equations. The result of this exercise is the following pair of equations:

$$1 = X_0^2 + 2X_0[\mathbf{c}_0(t)\cdot\tilde{\mathbf{c}}_0(t+\delta t)] + [\tilde{\mathbf{c}}_0(t+\delta t)\cdot\tilde{\mathbf{c}}_0(t+\delta t)] - \sum_{i=1}^{N} X_i^2 \tag{17a}$$

$$X_{i\neq 0} = -\tilde{\mathbf{c}}_0(t+\delta t)\cdot\mathbf{c}_i \tag{17b}$$

Equation 17b can be solved for $X_i$, for each $i > 0$, and then eq 17a affords $X_0$. To obtain $Y_i$, we first obtain velocity constraints by differentiating eqs 16a and 16b with respect to $t$ and then substitute the final velocity update, eqs 13a and 13b, into these velocity constraints. The result is

$$Y_i = -\dot{\tilde{\mathbf{c}}}_0(t+\delta t)\cdot\mathbf{c}_i(t+\delta t) \tag{18}$$

In deriving eqs 17a and 17b, we have assumed that the constraints are satisfied at time $t$, and in obtaining eq 18, we have assumed that the position constraints (eqs 16a and 16b) are satisfied at time $t + \delta t$. In practice, this means that the dynamics *cannot* start from a vector $\mathbf{c}_0$ that does not satisfy the constraints in eqs 16a and 16b. At the beginning of the annealing procedure for a particular state, the guess vector must be orthogonalized against all previously obtained vectors.

## III. COMPUTATIONAL DETAILS

We compute the optical absorption spectrum of the bulk hydrated electron under periodic boundary conditions, using Ewald summation for the long-range interactions.[5] Two hundred geometries were taken from a ground-state MD run in a periodic box that is 26.2015 Å on a side and contains 600 water molecules, corresponding to a density of 0.997 g/cm$^3$. We solve the Schrödinger equation on a grid with a spacing of 0.93 Å, for a total of $28^3$ = 21 952 grid points. Details of the simulation protocol can be found in ref 5.

The zeroth-order states are obtained with the Davidson−Liu method,[23] using a convergence threshold $\|(\hat{H}-E)\psi\| < 10^{-8}$ $E_h$ as described in ref 13. We use these zeroth-order states to generate a guess for the induced dipoles, $\{\vec{\mu}_i\}$, which we use to construct a Hamiltonian matrix. We then "anneal" the state of interest, subject to the constraint that it remain normalized and orthogonal to the previously determined states, as described above. Prior to initiation of the MD procedure, we orthogonalize the state of interest against all previous states, using the Gram−Schmidt procedure, so that the constraints are satisfied initially. The initial velocities ($\dot{\mathbf{c}}_0$) are taken to be zero. The electronic degrees of freedom quickly pick up kinetic energy since the guess vector is rarely near a minimum. Annealing proceeds until the change in energy between successive MD steps is less than $10^{-8}$ $E_h$. (By that point, the total electronic kinetic energy is also $\sim 10^{-8}$ $E_h$.) At this point we have an updated wave function that we use to induce new dipoles. This procedure is repeated until the energy change between successive dipole updates is less than $10^{-8}$ $E_h$.

In a typical CPMD calculation, one has to choose the fictitious electron mass and time step in such a way that the electronic degrees of freedom are adiabatically decoupled from the nuclear dynamics. (See refs 24−26 for an interesting discussion in the context of extended-Lagrangian MD.) This is not an issue here, as we are not propagating the nuclei; rather, we are trying to *find* the Born−Oppenheimer surface, not propagate dynamics along or near it. For this reason, we simply choose a time step and an electronic mass such that the annealing is stable. We use $\delta t$ = 0.1 fs and $\tilde{m}_{el}$= 400 au, but we have not attempted to optimize these parameters. (We do find that for $\delta t$ = 0.1 fs, masses less than 200 au lead to a failure to maintain the constraints.) In our calculations, the position and the velocity constraints are typically satisfied to an average absolute error of $10^{-14}$ and $10^{-16}$ au, respectively.

The friction parameter, $\gamma$, is chosen according to the recommendation in ref 27, which is based on a three-point fit using energies from successive steepest-decent steps. Since the initial wave function guess may be far from the minimum, we found it helpful to generate $\gamma$ several times during the MD routine; we do this every 50 time steps. We find that the annealing typically converges after 20−300 time steps if the guess is reasonable. However, in cases where the guess is poor, it may take upward of 2000 steps. The Hamiltonian is not updated during this procedure, so the annealing steps are quite inexpensive compared to inducing new dipoles and updating the potential energy at each grid point.

Below, we will compare the $e^-$(aq) spectrum obtained from the annealing procedure to that calculated using the perturbative scheme that was described in Section II. In the latter scheme, we do not allow the perturbed wave function to mix with the ground state, so that each perturbed state remains orthogonal to the ground state, even though the excited-state wave functions are not mutually orthogonal. (This at least ensures that the transition dipoles are translationally invariant.) An electronic spectrum is constructed from a histogram of oscillator strengths

$$f_{0\rightarrow n} = \frac{2m_e}{3\hbar^2}(E_n - E_0)\sum_{\kappa\in\{x,y,z\}}|\langle\psi_0|\hat{\kappa}|\psi_n\rangle|^2 \tag{19}$$

Wave functions were visualized with the Visual Molecular Dynamics program,[28] and isocontour values were generated with OpenCubMan.[29] Calculations were performed with a simulation code that is described in refs 5 and 13.

## IV. RESULTS

**A. Benchmark Tests Using Fixed Dipoles.** Prior to applying our procedure to determine the fully relaxed excited states of the aqueous electron, we would first like to demonstrate the method's effectiveness in the case that the induced dipoles are not updated. That is, we will first verify that the annealing procedure reproduces the lowest few eigenstates of a Hamiltonian where the induced dipoles are converged to the ground-state wave function (only), in which case there is no orthogonality problem. For this test, we first determine the ground-state wave function and induced dipoles with our standard method,[5,13] then solve for

the lowest 30 eigenstates of $\hat{H}$ with fixed dipoles. Next, we take a set of vectors composed of random numbers and use these as initial guess vectors for the annealing algorithm, fixing the induced dipoles at the values previously determined for the ground-state wave function.

Table I shows that the annealing procedure reproduces—with high accuracy—both the excitation energies and the oscillator strengths that are obtained by a straightforward Davidson−Liu procedure. In this particular case, where the dipoles are fixed, the states emerge from the annealing procedure in ascending order of energy, indicating that the procedure does not become trapped in any local minima and most likely locates *global* minima of the constrained optimization problem. (Of course, there is no guarantee that this will be the case once we allow the dipoles to relax.) Using the convergence thresholds specified in Section III, we can reproduce excitation energies to within $\sim 10^{-4}$ eV, which is far smaller than the error intrinsic to the pseudopotential model. Due to the completely random nature of the initial guesses, the annealing procedure takes ~1500 steps to converge in this example.

**Table I. Excitation Energies (in eV) and Oscillator Strengths, in the Absence of Dipole Relaxation, Computed Using Two Different Algorithms**

| | Davidson−Liu diagonalization | | electronic annealing | |
|---|---|---|---|---|
| $n$ | $E_n - E_0$ | $f_{0\to n}$ | $E_n - E_0$ | $f_{0\to n}$ |
| 1 | 2.13004 | 0.294897 | 2.13009 | 0.294889 |
| 2 | 2.22616 | 0.306758 | 2.22618 | 0.306793 |
| 3 | 2.45889 | 0.271951 | 2.45890 | 0.272044 |
| 4 | 2.89899 | 0.002009 | 2.89901 | 0.001878 |
| 5 | 3.35058 | 0.007256 | 3.35084 | 0.007513 |
| 6 | 3.36738 | 0.001328 | 3.36724 | 0.001038 |
| 7 | 3.42538 | 0.000995 | 3.42542 | 0.001048 |
| 8 | 3.47247 | 0.010379 | 3.47247 | 0.010336 |
| 9 | 3.57655 | 0.000950 | 3.57662 | 0.000979 |
| 10 | 3.62341 | 0.006859 | 3.62349 | 0.006142 |

Because the annealing procedure employs a larger number of constraints for higher-energy states as compared to lower-energy states, one might question whether the accuracy of the computed energies degrades as one marches up the manifold of states, adding more and more constraints as the calculation proceeds. The data in Table I suggest that this is not the case. For example, the $n = 8$ excitation energy computed by means of the annealing algorithm is closer to the Davidson−Liu result than is the $n = 1$ excitation energy. The accuracy is not degraded because the annealing algorithm does not introduce any *new* constraints beyond those imposed by linear algebra. For a fixed set of dipoles, the exact (nondegenerate) eigenvectors of the Hamiltonian are necessarily orthogonal, and obtaining them via diagonalization or via Davidson's procedure is equivalent to minimizing the Rayleigh−Ritz quotient

$$R[\psi] = \frac{\langle\psi|\hat{H}|\psi\rangle}{\langle\psi|\psi\rangle} \tag{20}$$

subject to the constraint that $|\psi_n\rangle$ must be orthogonal to all lower-lying states, $|\psi_0\rangle$, ..., $|\psi_{n-1}\rangle$. Our annealing algorithm simply provides an alternative means to enforce these constraints and to carry out the Rayleigh-Ritz variational procedure in a robust way.

Unlike this benchmark test involving fixed dipoles, the "right" answer is no longer well-defined once we let the MM dipoles relax. However, the very close agreement between the annealing results and the Davidson−Liu results in this test gives us confidence that our approach is a reasonable one, if one insists (as we do here) that the relaxed wave functions should be orthogonal to one another.

The excited states need not emerge in energetic order once we allow the induced dipoles to relax. They would do so only if the annealing procedure managed to find the global minimum of the effective potential (with constraints) on each annealing cycle. The presence of inducible dipoles appears to make this quite challenging, as the states do not come out of the calculations in ascending order. This gives us some pause and calls into question the nature of our guess. We have run additional calculations in which the guess for the annealing procedure is provided by the

**Table II. Excitation Energies (in eV) and Oscillator Strengths Computed by Electronic Annealing, Using Two Different Initial Guesses**

| | ordered by $n$[a] | | | | ordered by energy[b] | | | | | |
|---|---|---|---|---|---|---|---|---|---|---|
| | zeroth-order guess | | first-order guess | | zeroth-order guess | | first-order guess | | difference[c] | |
| $n$ | $E_n - E_0$ | $f_{0\to n}$ | $E_n - E_0$ | $f_{0\to n}$ | $E_n - E_0$ | $f_{0\to n}$ | $E_n - E_0$ | $f_{0\to n}$ | $E_n - E_0$ | $f_{0\to n}$ |
| 1 | 1.73894 | 0.133993 | 1.73894 | 0.133927 | 1.73894 | 0.133993 | 1.73894 | 0.133927 | 0.00000 | 0.000066 |
| 2 | 1.95139 | 0.237197 | 1.95140 | 0.237188 | 1.93676 | 0.028331 | 1.93668 | 0.028360 | 0.00008 | 0.000029 |
| 3 | 1.93676 | 0.028331 | 1.93668 | 0.028360 | 1.95139 | 0.237197 | 1.95140 | 0.237188 | 0.00001 | 0.000029 |
| 4 | 2.10816 | 0.132911 | 2.10817 | 0.132922 | 2.10816 | 0.132911 | 2.10817 | 0.132922 | 0.00001 | 0.000011 |
| 5 | 2.11486 | 0.001157 | 2.28370 | 0.001407 | 2.11486 | 0.001157 | 2.11521 | 0.001104 | 0.00035 | 0.000053 |
| 6 | 2.28397 | 0.001359 | 2.11521 | 0.001104 | 2.15224 | 0.000537 | 2.14726 | 0.000641 | 0.00498 | 0.000104 |
| 7 | 2.46492 | 0.001676 | 2.26762 | 0.004268 | 2.26925 | 0.004114 | 2.26762 | 0.004268 | 0.00163 | 0.000154 |
| 8 | 2.26925 | 0.004114 | 2.14726 | 0.000641 | 2.28397 | 0.001359 | 2.28370 | 0.001407 | 0.00027 | 0.000048 |
| 9 | 2.42928 | 0.001936 | 2.43138 | 0.001780 | 2.36290 | 0.003176 | 2.36278 | 0.003178 | 0.00012 | 0.000002 |
| 10 | 2.15224 | 0.000537 | 2.36278 | 0.003178 | 2.42928 | 0.001936 | 2.43138 | 0.001780 | 0.00210 | 0.000156 |
| 11 | 2.36290 | 0.003176 | 2.46681 | 0.001478 | 2.46492 | 0.001676 | 2.46681 | 0.001478 | 0.00189 | 0.000198 |

[a] Excitation energies listed in the order that the states are generated by the annealing procedure. [b] Excitation energies listed in ascending order of energy. [c] Difference in energies and oscillator strengths for the energy-ordered states computed using two different initial guesses.

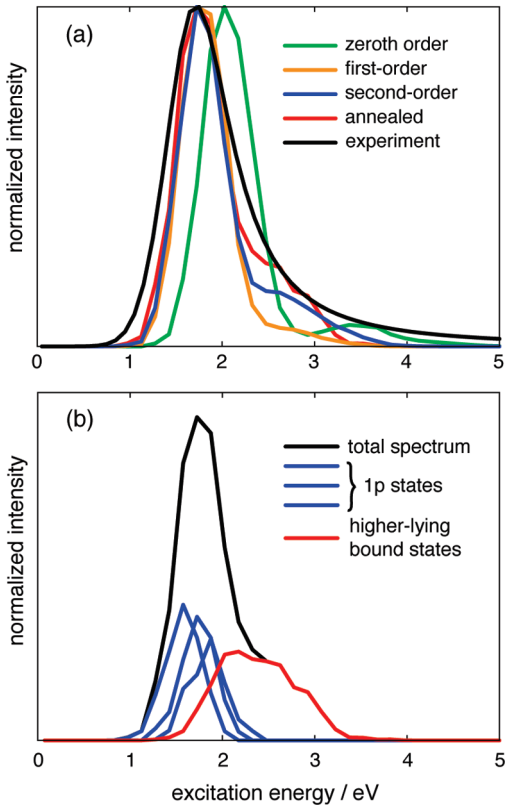


**Figure 1.** Absorption spectra for $e^-(aq)$ in bulk water: (a) comparison of spectra computed using zeroth-, first-, and second-order perturbative treatments of the $\hat{W}_n$ (eq 4) to the spectrum computed using the annealing procedure proposed here; and (b) decomposition of the annealed spectrum into contributions from various types of excited states.

first-order corrected wave function from the perturbative scheme. Inspection of the energies and oscillator strengths indicates that typically, the first four states are identical and emerge in the same order for either initial guess. Table II shows a typical case. The first four excitation energies are nearly identical for either initial guess and emerge in the same order, but the ordering is different starting with $n = 5$. However, both initial guesses do find the same set of excitation energies through at least $n = 11$.

The fact that the states do not come out energetically ordered is worrisome because the constraints placed on a particular state depend upon the order in which it is determined, and this should effect the energy. In the latter columns of Table II we have reordered the states energetically, and tabulated the differences in excitation energies and oscillator strengths between the two different initial guesses. The largest discrepancy in the energies between the two initial guesses is only 0.005 eV. This is smaller than the typical energy gap between states, and we therefore find this to be a tolerable error. In principle, one could probably ensure energetic ordering by annealing the same state several times, starting from a variety of different guesses and taking the lowest energy result in an attempt to find the global minimum for each set of constraints. Another possibility would be to perform the annealing, reorder the states energetically, and repeat the entire procedure using the annealed states as guesses. We have not done so here, owing to the smallness of the discrepancies between energies obtained using different initial guesses.

**B. Aqueous Electron Absorption Spectrum.** Figure 1a compares the absorption spectrum obtained using perturbative techniques[5] to that obtained using the annealing algorithm that is described here. The experimental spectrum (reproduced from the line shape parameters in ref 30) is also shown. With the exception of the annealed spectrum, which is new, these spectra have been described in detail in our previous work,[3−5] but for completeness, we briefly summarize these results here. At zeroth-order in the perturbation, the peak intensity is blue-shifted relative to experiment, and although this zeroth-order spectrum does reproduce the main, Gaussian feature in the experimental spectrum, it exhibits a gap in intensity just below 3 eV, which is followed by a "hump" centered around 3.5 eV that is essentially a photoelectron spectrum. The first-order correction for $\hat{W}_n$ shifts the maximum into quantitative agreement with experiment and also binds states that were (vertically) unbound at zeroth order, meaning that the excitation energies were greater than the vertical detachment energy. A second-order treatment of $\hat{W}_n$ affords a correction to the wave function and hence the transition dipoles, and this has the effect of increasing intensity in the "blue tail".

The spectrum obtained from electronic annealing agrees quantitatively with the second-order perturbation theory spectrum in the Gaussian region, but the annealing procedure shifts even more oscillator strength into the higher-lying bound states that comprise the blue tail. (All of the spectra in Figure 1 are normalized to unit intensity at their respective absorption maxima.) If anything, the blue tail in the annealed spectrum is in better agreement with experiment than is the second-order perturbation theory result.

Figure 1b decomposes the annealed spectrum into contributions from 1s → 1p transitions versus excitations into higher-lying bound states. The 1p states are the only bright states, for an aqueous electron modeled as a particle in a spherical box,[3] and indeed the 1s → 1p excitations carry much of the oscillator strength in the annealed spectrum. However, the 1p band has significant energetic overlap with the higher-lying bound states, which borrow intensity from the 1p states and give rise to a significant "blue tail". The states that comprise this tail are unbound in the zeroth-order treatment, and we have previously referred to them as "quasi-continuum, polarization-bound" excited states.[4] These states have very little oscillator strength at zeroth order, but relaxation of the solvent dipoles allows them to mix with (and borrow intensity from) the 1p states. For the annealed spectrum, all 30 states that we calculate are vertically bound. (The average vertical binding energy for the simulation cell used in this work is 3.35 eV,[5] well into the blue tail in the spectra shown in Figure 1.)

At zeroth-order in $\hat{W}_n$ (what we have previously called the "unrelaxed" approximation),[4,5,3] the states are ordered as follows. The ground state is spherical (1s) and resides in a roughly spherical solvent cavity, while the first three excited states are p-like (1p). The fourth excited state is typically more diffuse and can be identified as the 2s state by virtue of a radial node. Above the 2s state are several states that resemble 1d states, but above this it becomes difficult to assign particle-in-a-cavity quantum numbers to the excited states, whose wave functions are quite diffuse and contain many different lobes. The qualitative nature of these states is not altered significantly by application of second-order perturbation theory.

The annealing procedure, on the other hand, sometimes *does* alter the initial guess wave functions in a qualitative way. In

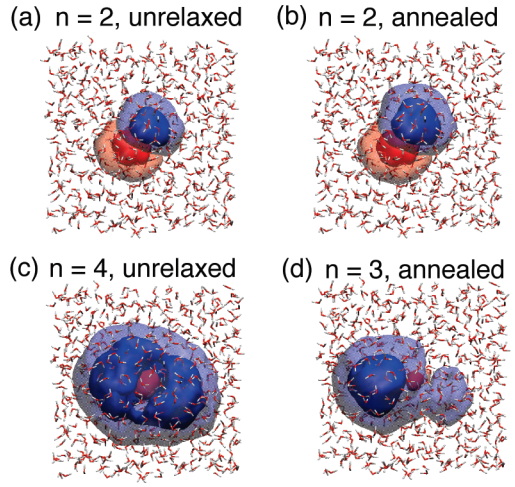


**Figure 2.** Examples of 1p- and 2s-like excited states of the aqueous electron. Panels (a) and (c) depict the "unrelaxed" states (zeroth order in $\hat{W}_n$), while panels (b) and (d) depict the wave functions that are obtained by electronic annealing. The opaque and translucent isosurfaces encapsulate 70% and 95% of $|\psi|^2$, respectively.

particular, the annealing procedure appears to have the ability to localize diffuse electronic states composed of largely disjoint lobes and in some cases may enhance the oscillator strength associated with these states, relative to the nominal bright states. In cases where we observe such localization, the nodal character of the state appears to be preserved, although this is only evident if the wave function is plotted using an isosurface that encapsulates nearly all of the electron density.

As an example, Figure 2 depicts the unrelaxed $n = 2$ and $n = 4$ wave functions from the calculation reported in Table I as well as the corresponding annealed wave functions from the calculation reported in Table II. (The states are labeled in the order that they are calculated by the annealing procedure, which need not be in energetic order.) The unrelaxed 1p state shown in Figure 2a is not altered by the annealing process in any substantive way and is nearly identical to the $n = 2$ state in the manifold of annealed excited states (Figure 2b). However, the annealed analogue (Figure 2d) of the $n = 4$ zeroth order wave function (Figure 2c) is more localized than its counterpart. The annealed function appears p-like rather than s-like, if a large isosurface contour value is used to plot the wave function. However, a smaller contour that encapsulates more of the wave function reveals s-like character. The transition from the unrelaxed to the annealed wave function ( i.e., Figure 2c⟶d) enhances the transition dipole of the state in question, because the localized, annealed state has better overlap with the ground state and furthermore sheds some of the pseudo-s-type symmetry that causes the unrelaxed state in Figure 2c to exhibit a rather small oscillator strength.

Comparison of Tables I and II seems to indicate that the $n = 3$ state loses significant oscillator strength upon annealing, but an inspection of the wave functions reveals that the state that emerges as $n = 3$ from the annealing procedure actually corresponds to the *fourth* excited state at zeroth-order. The latter acquires significant oscillator strength upon annealing and drops below a state with p-type character to become $n = 3$. While this sort of reordering does not occur in the majority of the cases, it is also not entirely uncommon.

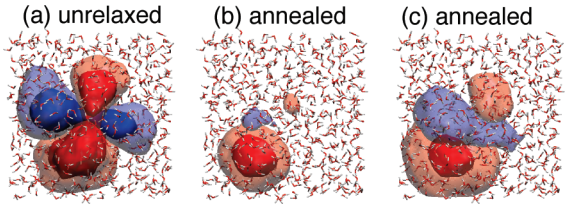


**Figure 3.** An excited electronic state of the aqueous electron with d-type character. Panels (a) and (b) depict the zeroth-order (unrelaxed) and annealed wave functions, respectively, using opaque and translucent isosurfaces that encapsulate 70% and 95% of $|\psi|^2$, respectively. Panel (c) depicts the same annealed wave function as in (b) but plotted using isosurfaces that encapsulate 70% and 99% of $|\psi|^2$.

From the spectrum in Figure 1b, it appears that the highest-lying 1p state carries somewhat less intensity than the two lower-lying 1p states. This is partly an artifact of the manner in which we analyzed the data, namely, we assumed in constructing Figure 1b that the first three states are the 1p states, which is always true in the perturbative approach but is occasionally *not* true following annealing. Despite this occasional reordering of states, the 1p states still carry the vast majority of the oscillator strength and are still responsible for the Gaussian feature in the absorption spectrum.

Figure 3 shows the zeroth-order and the annealed wave functions for a d-type state. Using an isosurface that encapsulates 90% of $|\psi|^2$ (Figure 3b), it appears as though the annealed state is effectively a "charge hop", in which the electron is transferred a sizable distance away from the cavity in which the ground-state wave function is localized. However, Figure 3c depicts the same annealed wave function, plotted using an isosurface that encapsulates 99% of $|\psi|^2$. In the latter depiction, it is clear that the wave function remains d-like, but the electron has largely localized into one of the lobes. In this example, the annealed state has very little overlap with the ground state, which results in a very small transition dipole. States that have localized to such an extent as to exhibit charge-transfer or charge-hopping character exhibit very small oscillator strengths and thus do not contribute greatly to the absorption spectrum. These states are most likely not accessed in experiments that probe vertically excited states. The "blue tail" does not arise from localized charge-hopping states, such as that shown in Figure 3b and c. Rather, it arises due to higher-lying, diffuse excited states that do have reasonable overlaps with the ground-state wave function.[4,5]

## V. DISCUSSION

According to the Thomas−Reiche−Kuhn (TRK) sum rule[31]

$$\sum_{n>0} f_{0\rightarrow n} = N_e \tag{21}$$

where $N_e$ is the number of electrons. By construction, $N_e = 1$ in our pseudopotential model. In previous work,[5] we observed that $f_{0\rightarrow 1} + f_{0\rightarrow 2} + \cdots + f_{0\rightarrow 29} \approx 0.95$ at zeroth-order, that is, the first 29 excited states account for 95% of the total oscillator strength. A first-order correction for $\hat{W}_n$ reduces the electronic energy gaps $(E_n - E_0)$ but does not affect the wave functions, and as a result, the total oscillator strength carried by the first 29 excited states is reduced to ≈0.8. At second order, the wave function *is* corrected, and the total oscillator strength recovers, to ≈0.9. In the present treatment, however, we find that $f_{0\rightarrow 1} + \cdots + f_{0\rightarrow 29} \approx 0.65$.

The question then arises as to whether the TRK sum rule is preserved in the case of a state-dependent Hamiltonian and whether or not the expression for $f_{0\rightarrow n}$ in eq 19 is even valid in such a case. Here, we address these questions in the context of the proposed annealing procedure.

In principle, the annealing procedure provides a way to obtain an infinite number of mutually orthogonal states, each of which is an eigenfunction of a different Hamiltonian. For the purpose of analyzing the sum rule in eq 21, let us make the (perhaps dubious) assumption that this set of eigenfunctions forms a complete orthonormal basis. Then to derive eq 21, one employs the identity:

$$[\hat{H}, \hat{x}] = -\frac{i\hbar}{m}\hat{p}_x \tag{22}$$

In principle, $\hat{H}$ could be any of the aforementioned Hamiltonians. Inserting eq 22 into the expression

$$\frac{1}{i\hbar}\langle 0|[\hat{x}, \hat{p}_x]|0\rangle = 1 \tag{23}$$

and using a resolution of the identity, one obtains

$$\frac{m}{\hbar^2}\sum_n [\langle 0|\hat{x}|n\rangle\langle n|[\hat{H}, \hat{x}]|0\rangle - \langle 0|[\hat{H}, \hat{x}]|n\rangle\langle n|\hat{x}|0\rangle] = 1 \tag{24}$$

This equation is valid for any Hamiltonian and any complete orthonormal basis. However, in order to obtain the sum rule in eq 21 from eq 24, the basis states $|n\rangle$ must in addition be eigenstates of the *same* Hamiltonian. In the present case, however, each state is a solution to a different Hamiltonian so the sum rule is not preserved by the annealing procedure. (As such, nothing rests upon our dubious assumption that the states $|n\rangle$ form a complete basis; the sum rule is not preserved, whether or not this is in fact the case.)

Next, we address the question of whether or not eq 19 is a valid formula for computing absorption intensities. In what follows, we assume that the nuclei are clamped, and we consider the electronic dynamics. The oscillator strength formula in eq 19 follows from time-dependent perturbation theory.[31] If the system is in state $|n\rangle$ at time $t = 0$, then it seems reasonable that the system evolves under the influence of the Hamiltonian for state $|n\rangle$, $\hat{H}_n$. That is,

$$|\Psi(t)\rangle = e^{-i\hat{H}_n t/\hbar}|n\rangle = e^{-iE_n t/\hbar}|n\rangle \tag{25}$$

where we have used the fact that $\hat{H}_n|n\rangle = E_n|n\rangle$.

We now investigate the time evolution in the presence of a time-dependent perturbation. We assume that the time-dependent wave function can be written

$$|\Psi(t)\rangle = \sum_n c_n(t)e^{-iE_n t/\hbar}|n\rangle \tag{26}$$

This expansion may seem suspicious in light of questions regarding whether the basis $\{|n\rangle\}$ is complete. However, we assume below that the system is initially in the ground state, and we are only interested in the dynamics within the finite subset of states that we have determined by means of annealing. In other words, this basis constitutes the region of interest in Hilbert space. To derive a formula for the transition probabilities, the ansatz in eq 26 should next be inserted into the time-dependent Schrödinger equation, but with which Hamiltonian? In the weak-field limit, the traditional assumption is that the system occupies the ground state at $t = 0$, $c_n(0) = \delta_{n,0}$. It therefore seems reasonable to assume that the dynamics is governed by the ground-state Hamiltonian, so that

$$i\hbar|\dot{\Psi}(t)\rangle = (\hat{H}_0 + V(t))|\Psi(t)\rangle \tag{27}$$

These assumptions, together with the fact that the basis is orthonormal, lead to the textbook[31] dynamical equations for the expansion coefficients $c_n(t)$. For this reason, we would argue that eq 19 is still valid, even though the TRK sum rule is not.

The ambiguity regarding which Hamiltonian guides the dynamics of the system is clearly an artifact of the model. The inducible dipoles represent electronic degrees of freedom and should respond on the time scale of electronic motion, i.e., these degrees of freedom participate in the short-time dynamics that results in absorption of radiation, and they ought to be included in the quantum mechanical description of the system. Our decision to treat some of the electronic variables (solvent dipoles) classically leads to some ambiguity (multiple Hamiltonians) since we do not have information regarding the short-time quantum dynamics of these variables. This is to be contrasted with the MOM-SCF technique[14,15] that was mentioned in Section I. In that method, there is a single Hamiltonian but multiple stationary points (solutions to the SCF equations). Since the SCF energy, at least in Hartree−Fock theory, is the expectation value of the true Hamiltonian, there is no ambiguity as to the quantum dynamics.

In the case of the methodology pursued here, one way around these difficulties would be to use a linear-response formalism, which has been explored in the context of time-dependent density functional theory (TD-DFT) in the presence of a polarizable medium.[32,33] Here, however, we were interested in a self-consistent, nonperturbative approach. In the future, it might be interesting to compare results obtained from linear-response theory to those obtained from our electronic annealing procedure.

Finally, we would like to speculate that this annealing procedure might be useful for MOM-SCF calculations. The MOM-SCF method appears quite promising and avoids some problems associated with TD-DFT. However, the excited-state wave functions obtained in MOM-SCF calculations are not orthogonal, although preliminary results do not seem to exhibit any adverse effects on oscillator strengths, possibly because the deviations from orthogonality are small in cases examined so far.[14] In any case, it is possible that the sort of electronic annealing that is introduced here could eliminate any concern over oscillator strengths. This technique might also be useful in the context of excited-state Kohn−Sham simulations,[34] nonadiabatic (surface hopping) simulations utilizing CPMD,[35] or "constrained" DFT calculations,[36,37] each of which is potentially subject to nonorthogonality problems. Extensions to many-electron QM/MM methods using polarizable force fields are also worth exploring.

## VI. SUMMARY

We have introduced a novel "electronic annealing" procedure that is capable of finding orthogonal solutions to a state-dependent Hamiltonian. This procedure appears to be robust and is capable of finding many such solutions. When applied to a polarizable QM/MM model of the aqueous electron in bulk water,[5] the electronic absorption spectrum computed by means of electronic annealing is in reasonable agreement with results obtained previously[4,5] based on a perturbative treatment of the

MM polarization response following excitation of the QM region. In fact, the annealed spectrum is in slightly better agreement with experiment, as compared to perturbative results. In any case, these computed spectra all support the hypothesis that electronic polarization (as described theoretically via atom-centered inducible dipoles) binds additional excited states of the aqueous electron and facilitates intensity borrowing from the 1p states that carry most of the oscillator strength. The "blue tail" in the optical spectrum of $e^-(aq)$ arises from what we have termed "polarization-bound quasi-continuum states".[4] Here, we find that electronic reorganization of the solvent can also cause diffuse excited states of the electron to localize into "charge-hopping" states. These excitations, however, carry very little oscillator strength and do not make a substantial contribution to the optical absorption spectrum.

In the future, we plan to explore generalizations of this electronic annealing algorithm that are suitable for many-electron QM calculations.

## AUTHOR INFORMATION

### Corresponding Author

*E-mail: herbert@chemistry.ohio-state.edu.

## ACKNOWLEDGMENT

We thank Xiaosong Li for encouraging us to complete and submit this paper. This work was supported by a National Science Foundation CAREER award (CHE-0748448). Calculations were performed at the Ohio Supercomputer Center under project no. PAS-0291. L.D.J. acknowledges a Presidential Fellowship from The Ohio State University. J.M.H. is an Arthur P. Sloan Foundation Fellow and a Camille Dreyfus Teacher−Scholar.

## REFERENCES

(1) Hart, E. J.; Boag, J. W. *J. Am. Chem. Soc.* **1962**, *84*, 4090–4095.
(2) Mostafavi, M.; Lampre, I. In *Radiation Chemistry*; Spotheim-Maurizot, M., Mostafavi, M., Belloni, J., Douki, T., Eds.; EDP Sciences: Les Ulis Cedex A, France, **2008**; Chapter 3, pp 33−52.
(3) Herbert, J. M.; Jacobson, L. D. *Int. Rev. Phys. Chem.* **2011**, *30*, 1–48.
(4) Jacobson, L. D.; Herbert, J. M. *J. Am. Chem. Soc.* **2010**, *132*, 10000–10002.
(5) Jacobson, L. D.; Herbert, J. M. *J. Chem. Phys.* **2010**, *133*, 154506:1–19.
(6) Schnitker, J.; Rossky, P. J. *J. Chem. Phys.* **1987**, *86*, 3462–3470.
(7) Barnett, R. N.; Landman, U.; Cleveland, C. L.; Jortner, J. *J. Chem. Phys.* **1988**, *88*, 4421–4428.
(8) Turi, L.; Gaigeot, M.-P.; Levy, N.; Borgis, D. *J. Chem. Phys.* **2001**, *114*, 7805–7815.
(9) Sommerfeld, T.; DeFusco, A.; Jordan, K. D. *J. Phys. Chem. A* **2008**, *112*, 11021–11035.
(10) Garrett, B. C.; Dixon, D. A.; Camaioni, D. M.; Chipman, D. M.; Johnson, M. A.; Jonah, C. D.; Kimmel, G. A.; Miller, J. H.; Rescigno, T. N.; Rossky, P. J.; Xantheas, S. S.; Colson, S. D.; Laufer, A. H.; Ray, D.; Barbara, P. F.; Bartels, D. M.; Becker, K. H.; Bowen, K. H., Jr.; Bradforth, S. E.; Carmichael, I.; Coe, J. V.; Corrales, L. R.; Cowin, J. P.; Dupuis, M.; Eisenthal, K. B.; Franz, J. A.; Gutowski, M. S.; Jordan, K. D.; Kay, B. D.; LaVerne, J. A.; Lymar, S. V.; Madey, T. E.; McCurdy, C. W.; Meisel, D.; Mukamel, S.; Nilsson, A. R.; Orlando, T. M.; Petrik, N. G.; Pimblott, S. M.; Rustad, J. R.; Schenter, G. K.; Singer, S. J.; Tokmakoff, A.; Wang, L.-S.; Wittig, C.; Zwier, T. S. *Chem. Rev.* **2005**, *105*, 355–389.
(11) Buxton, G. V. In *Radiation Chemistry*; Spotheim-Maurizot, M., Mostafavi, M., Belloni, J., Douki, T., Eds.; EDP Sciences: Les Ulis Cedex A, France, **2008**; Chapter 1, pp 3−16.
(12) Ren, P.; Ponder, J. W. *J. Phys. Chem. B* **2003**, *107*, 5933–5947.
(13) Jacobson, L. D.; Williams, C. F.; Herbert, J. M. *J. Chem. Phys.* **2009**, *130*, 124115:1–18.
(14) Gilbert, A. T. B.; Besley, N. A.; Gill, P. M. W. *J. Phys. Chem. A* **2008**, *112*, 13164–13171.
(15) Besley, N. A.; Gilbert, A. T. B.; Gill, P. M. W. *J. Chem. Phys.* **2009**, *130*, 124308:1–7.
(16) Dupuis, M.; Aida, M.; Kawashima, Y.; Hirao, K. *J. Chem. Phys.* **2002**, *117*, 1242–1255.
(17) Car, R.; Parrinello, M. *Phys. Rev. Lett.* **1985**, *55*, 2471–2474.
(18) Marx, D.; Hutter, J. In *Modern Methods and Algorithms in Quantum Chemistry*, 2nd ed.; Grotendorst, J., Ed.; John von Neumann Institute for Computing: Jülich, Germany, 2000; Vol. 1 of NIC Series, pp 329−477.
(19) Tassone, F.; Mauri, F.; Car, R. *Phys. Rev. B* **1994**, *50*, 10561–10573.
(20) Allen, M. P.; Tildesley, D. J. *Computer Simulations of Liquids*; Oxford University Press: New York, 1992.
(21) Tuckerman, M. E.; Parrinello, M. *J. Chem. Phys.* **1994**, *101*, 1302–1315.
(22) Andersen, H. C. *J. Comput. Phys.* **1983**, *52*, 24–34.
(23) Murray, C. W.; Racine, S. C.; Davidson, E. R. *J. Comput. Phys.* **1992**, *103*, 382–389.
(24) Herbert, J. M.; Head-Gordon, M. *J. Chem. Phys.* **2004**, *121*, 11542–11556.
(25) Iyengar, S. S.; Schlegel, H. B.; Scuseria, G. E.; Millam, J. M.; Frisch, M. J. *J. Chem. Phys.* **2005**, *123*, 027101:1–2.
(26) Herbert, J. M.; Head-Gordon, M. *J. Chem. Phys.* **2005**, *123*, 027102:1–2.
(27) Probert, M. I. J. *J. Comput. Phys.* **2003**, *191*, 130–146.
(28) Humphrey, W.; Dalke, A.; Schulten, K. *J. Mol. Graphics* **1996**, *14*, 33–38.
(29) Haranczyk, M.; Gutowski, M. *J. Chem. Theory Comput.* **2008**, *4*, 689–693.
(30) Coe, J. V.; Williams, S. M.; Bowen, K. H. *Int. Rev. Phys. Chem.* **2008**, *27*, 27–51.
(31) McHale, J. L. *Molecular Spectroscopy*; Prentice Hall: Upper Saddle River, New Jersey, 1998.
(32) Yoo, S.; Zahariev, F.; Sok, S.; Gordon, M. S. *J. Chem. Phys.* **2008**, *129*, 144112:1–8.
(33) Steindal, A. H.; Ruud, K.; Frediani, L.; Aidas, K.; Kongsted, J. *J. Phys. Chem. B* **2011**, *115*, 3027–3037.
(34) Doltsinis, N. L.; Marx, D. *Phys. Rev. Lett.* **2002**, *88*, 166402:1–4.
(35) Tapavicza, E.; Tavernelli, I.; Rothlisberger, U. *Phys. Rev. Lett.* **2007**, *98*, 023001:1–4.
(36) Wu, Q.; Van Voorhis, T. *J. Chem. Theory Comput.* **2006**, *2*, 765–774.
(37) Wu, Q.; Cheng, C.-L.; Van Voorhis, T. *J. Chem. Phys.* **2007**, *127*, 164110:1–9.